The Geological Society of America
Special Paper 516
2015

Analysis of hydrologic and geochemical time-series data at James Cave, Virginia: Implications for epikarst influence on recharge in Appalachian karst aquifers

Sarah Eagle
Department of Geosciences, Virginia Tech, 1405 Perry Street, Blacksburg, Virginia 24061, USA

William Orndorff
Virginia Department of Conservation and Recreation, 600 E. Main Street, 24th Floor, Richmond, Virginia 23219, USA

Benjamin Schwartz
Department of Biology and Edwards Aquifer Research and Data Center, Texas State University, 601 University Drive, San Marcos, Texas 78666-4684, USA

Daniel H. Doctor
U.S. Geological Survey, 12201 Sunrise Valley Drive, MS 926A, Reston, Virginia 20192, USA

Jonathan Gerst
Madeline Schreiber*
Department of Geosciences, Virginia Tech, 1405 Perry Street, Blacksburg, Virginia 24061, USA

ABSTRACT

The epikarst, which consists of highly weathered rock in the upper vadose zone of exposed karst systems, plays a critical role in determining the hydrologic and geochemical characteristics of recharge to an underlying karst aquifer. This study utilized time series (2007–2014) of hydrologic and geochemical data of drip water collected within James Cave, Virginia, to examine the influence of epikarst on the quantity and quality of recharge in a mature, doline-dominated karst terrain. Results show a strong seasonality of both hydrology and geochemistry of recharge, which has implications for management of karst aquifers in temperate climatic zones. First, recharge (discharge from the epikarst to the underlying aquifer) reaches a maximum between late winter and early spring, with the onset of the recharge season ranging from as early as December to as late as March during the study period. The timing and duration of the recharge season were found to be a function of precipitation in

*Corresponding author: mschreib@vt.edu.

Eagle, S., Orndorff, W., Schwartz, B., Doctor, D.H., Gerst, J., and Schreiber, M., 2015, Analysis of hydrologic and geochemical time-series data at James Cave, Virginia: Implications for epikarst influence on recharge in Appalachian karst aquifers, *in* Feinberg, J., Gao, Y., and Alexander, E.C., Jr., eds., Caves and Karst Across Time: Geological Society of America Special Paper 516, doi:10.1130/2015.2516(15). For permission to copy, contact editing@geosociety.org.

excess of evapotranspiration on a seasonal time scale. Secondly, seasonally variable residence times for water in the epikarst influence rock-water interaction and, hence, the geochemical characteristics of recharge. Overall, results highlight the strong and complex influence that the epikarst has on karst recharge, which requires long-term and high-resolution data sets to accurately understand and quantify.

INTRODUCTION

The epikarst, also known as the subcutaneous zone, consists of highly weathered rock in the upper vadose zone of exposed karst systems. The epikarst connects the soil overburden to the underlying transmission zone, where conduits dominate the hydrology (Williams, 2008). In the epikarst, heterogeneities in hydraulic conductivity create the potential for transient storage of infiltrating water (Williams, 1983; Smart and Friederich, 1987; Klimchouk, 2003; Perrin et al., 2003; Bakalowicz, 2004; Aquilina et al., 2006; Williams, 2008) and the hydrologic and geochemical attenuation of infiltration, which influences the timing, rate, and quality of recharge to an underlying karst aquifer.

Historically, study of the epikarst has been difficult due to inherent complexity and instrumentation limitations (Williams, 2008). Over the past two decades, however, improvements in instrumentation and data logging have allowed automated collection of high-resolution hydrologic and geochemical time-series data in caves. Several studies have used such data sets to examine relationships between precipitation patterns and cave drip rates in different climatic regions, yielding important insights into the effects of seasonal and annual climate variations on karst aquifer recharge (e.g., McDonald and Drysdale, 2007; Pape et al., 2009; Sheffer et al., 2011). Other studies have combined drip rate and geochemical data sets to infer flow pathways within the epikarst (e.g., Genty and Deflandre, 1998; Tooth and Fairchild, 2003), and to examine how drip rates influence speleothem growth for paleoclimate interpretation (Fairchild et al., 2000; Tooth and Fairchild, 2003; Baldini et al., 2006; McDonald and Drysdale, 2007; Gregory et al., 2009; Sheffer et al., 2011). Continuous data sets have also been combined with collection of periodic samples for geochemical analysis, including trace elements (Fairchild et al., 2000), organic matter luminescence (Baker et al., 2000), isotopes (Musgrove and Banner, 2004; Pape et al., 2009), specific conductance (Genty and Deflandre, 1998), and P_{CO2} (Fairchild et al., 2000; Sherwin and Baldini, 2011; Baldini et al., 2012). For example, Musgrove and Banner (2004) used Sr isotopes, in combination with soil leachate, drip-water, and phreatic groundwater geochemistry, to infer residence times of water in the epikarst. Others have used Mg/Ca and Sr/Ca ratios to infer prior calcite precipitation in the vadose zone above the cave (e.g., Fairchild et al., 2000; Baldini et al., 2006; Fairchild and McMillan, 2007).

This study furthers these works by combining high-resolution hydrologic and geochemical data sets from a cave in southwestern Virginia to examine seasonal and annual variability in hydrology and geochemistry of epikarst discharge. Signals in a combined hydrogeochemical data set are interpreted and used to build a conceptual model of physical and chemical interactions in the epikarst. Results of this study can be extended to other doline-dominated karst systems with similar geology in temperate climates where precipitation is relatively constant throughout the year but evapotranspiration is highly seasonal and is most active from late spring through early fall.

SITE DESCRIPTION

James Cave is located in Pulaski County, Virginia, in a temperate climate zone. The county experiences a mean annual temperature of 11.4 °C and receives an average of 988 mm of precipitation per year (SERCC, 2012). Land use in the vicinity of the cave is dominantly agricultural, with cattle pasture and some row crops. The study region is in the Great Valley subprovince of the Appalachian Valley and Ridge physiographic province (Bingham, 1991). The Pulaski fault system dominates the structural geology in the region around the study site (Bartholomew, 1987; Schultz and Bartholomew, 2009). James Cave consists of ~2.3 km of cave passage formed nearly parallel to bedding strike in the Cambrian Conococheague Formation (Fig. 1). The cave's vertical extent is 39 m. An in-cave stream flows east toward the New River, which defines regional base level. Attempts to determine the resurgence for the cave stream using dye tracing have been unsuccessful to date (Joseph Fagan, Virginia Department of Conservation and Recreation, 2009, personal commun.).

Schultz and Bartholomew (2009) described the Conococheague section in the study area as 550–610 m of thick-bedded (0.9–1.4 m) sequences of basal intraformational limestone- and dolomite-clast conglomeratic limestone overlain by millimeter to centimeter laminated blue-gray limestone, in turn overlain by bluish-gray "ribbon" limestone, and capped by blocky, light-gray dolomite or pink, dolomitic mudstone. The sequences are interbedded with chert-bearing dark-gray stromatolitic limestone, light-pink limestone and dolomite, rippled and mud-cracked light-gray limestone and dolomite, and blocky dolomite and oolitic chert. Lenses of fine-grained, light-gray, 2.5–20.3-cm-thick carbonate-cemented quartz sandstones occur throughout the section.

Soils overlying the bedrock at the study site are mapped as Lowell silt loam and Wurno-Newbern-Faywood silt loam (USDA-NRCS, 2006), ranging in thickness from 0.25 to 2 m, with a carbonate regolith developed at the soil-bedrock interface. River terrace deposits, presumably Quaternary in age (Schultz and Batholomew, 2009), occur just south of the study area and

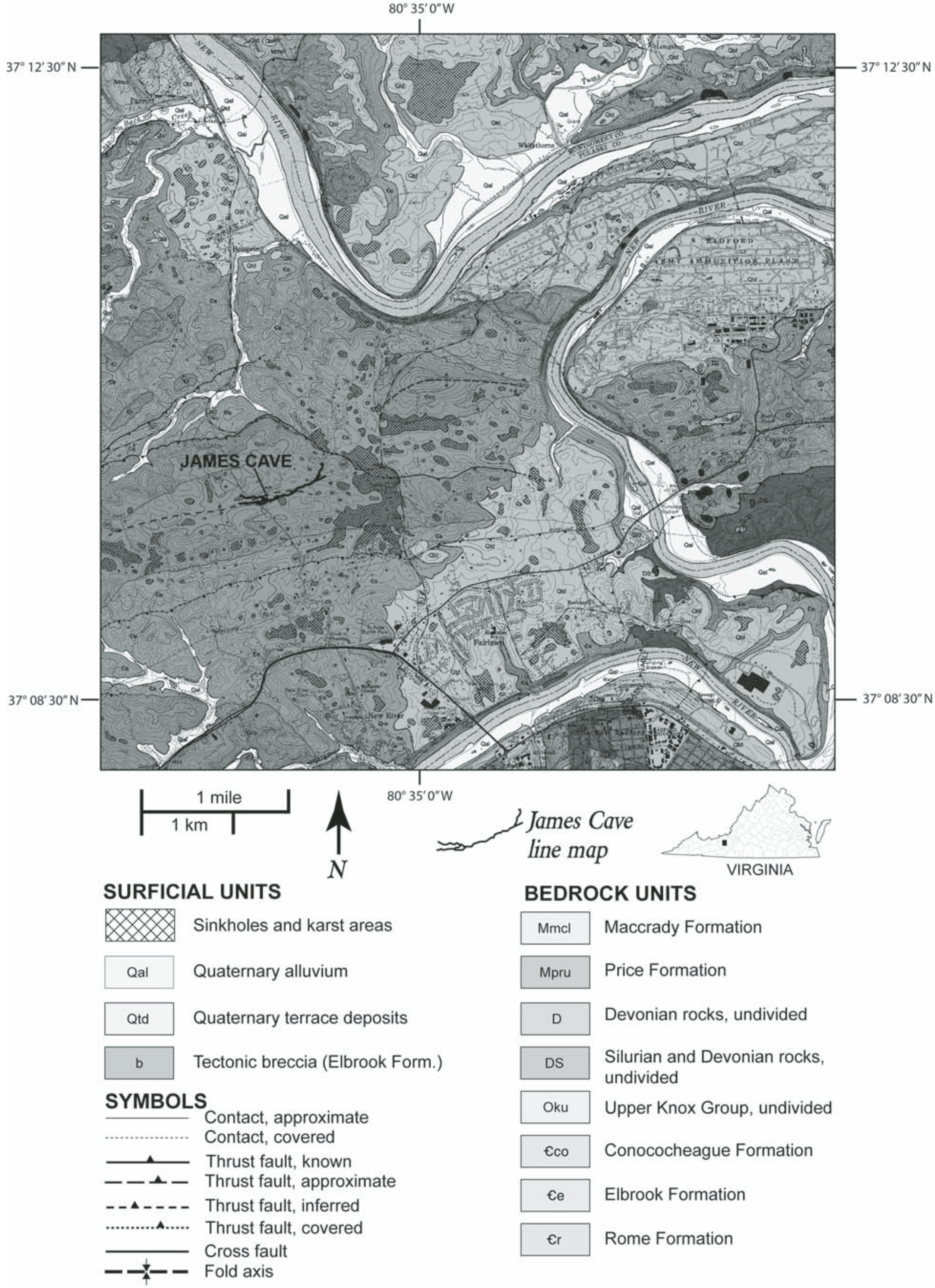

Figure 1. Geologic map of area surrounding James Cave. Geologic data are from Schultz and Bartholomew (2009). Line drawing of James Cave is from the National Speleological Society, provided courtesy of the Virginia Speleological Survey.

overlie the same bedrock with similar karst topography. These deposits may have extended over the study area in the past, as evidenced by well-rounded quartzite cobbles found locally on the surface and in the cave stream.

The style of karst in which James Cave is developed is best described as a doline karst, as defined by Field (2002), where surface topography is dominated by a high density of dolines (sinkholes), with no perennial surface streams and few defined channels. Water entering the cave mostly infiltrates through the epikarst, with some surface water runoff bypassing the epikarst via sinkholes. No perennial sinking streams have been identified in the watershed of James Cave.

METHODS

Site Instrumentation and Sampling Methods

Instrumentation of Monitoring Sites

Within James Cave, ceiling drip collectors were established at three actively dripping sites to measure the rate, temperature, and specific conductance of water draining from the overlying epikarst. Locations of the drip monitoring sites in the cave are shown in Figure 2. Drip collectors were installed where cave ceilings were within 15 m of the overlying land surface, which is within the known vertical range of the epikarst observed in most karst regions (Klimchouk, 2003). Monitoring stations 1 and 2 are ~10 m below land surface, while monitoring station 3 is at ~7 m depth. The drip collectors were built using plastic sheeting attached to a polyvinyl chloride (PVC) frame. Frames were suspended from the cave ceiling or wall, and the tarps drained to a low-volume reservoir in which specific conductance (SpC) and temperature of drip waters were measured with and stored on an Onset HOBO U24-001 (all trade names are used for identification purposes only and do not indicate endorsement by the U.S. Geological Survey). From the reservoir, drips drained into a tipping bucket rain gauge (Onset HOBO RGB-M002) to measure and log drip rates at 10 min intervals (Fig. 3). Drip rate data were stored on Micro Station data loggers (Onset HOBO H21-002).

On the surface, a weather station near the cave entrance measured precipitation using a tipping bucket rain gauge (Onset HOBO RGB-M002), and it also measured air temperature and relative humidity (Onset HOBO S-THB-M002). When possible, missing data due to weather station failure were replaced with data from the nearby Virginia Tech Kentland Experimental Farm (labeled "Whitethorne" in Fig. 1). Precipitation rate, air temperature, and relative humidity data were stored on a Micro Station data logger (Onset HOBO H21-002).

Data were retrieved from the instruments on a monthly or bimonthly basis. Time-series data were imported into AQUARIUS Workstation (AquaticInformatics, 2011), which was used to merge, process, correct, and resample, where necessary. Additional information on instrumentation, including details on maintenance and calibration, as well as data processing and management, is included in Eagle (2013) and Schreiber et al. (2015).

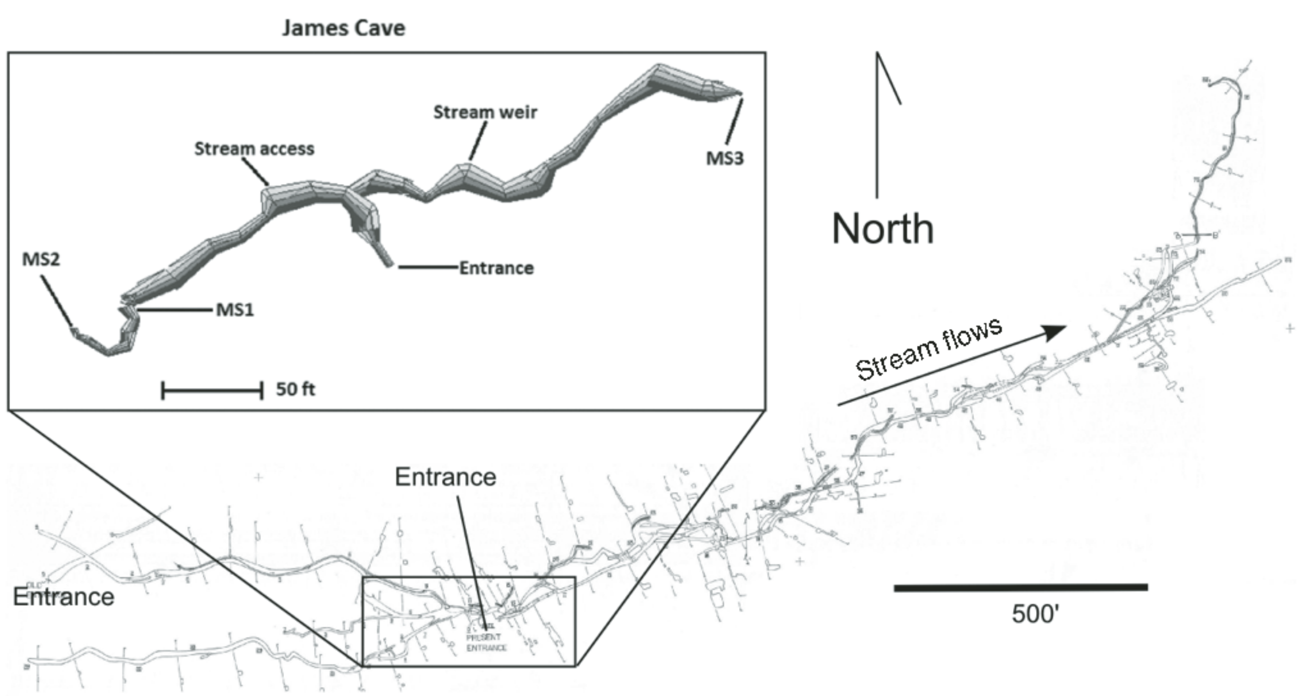

Figure 2. Survey of James Cave, courtesy of B. Lewis, E.F. Morgan, and the New River Valley Cave Club. Inset map shows locations of cave entrance and drip monitoring stations (MS1–MS3), courtesy of T. Malabad. *Note:* 50 ft = 15.25 m.

Geochemical Samples

Discrete and integrated samples of precipitation, soil water, and drip water were collected for geochemical analysis. Precipitation was captured using a funnel in which a circular float was placed to minimize evaporation (modeled after Kazahaya and Yasuhara, 1994). The funnel was channeled via tubing to the bottom of a sealed PVC pipe. The pipe was fitted with a coiled vent tube at the top to prevent evaporation.

In the shallow vadose zone, three tension lysimeters (Soil Moisture 1900L) installed at ~1 m depth allowed collection of soil water samples. Two of these were located over in-cave drip monitoring sites, and the third was located near the cave entrance, at the base of a sinkhole. The soil water samples were collected from the tension lysimeters using a manual vacuum pump.

Cave drip waters were continuously collected using composite sample containers fitted with an airlock and overflow (see Fig. 3). It should be noted that the time interval of these integrated drip samples varied based on drip rate. During high-flow periods, the sample from the container may have only represented a time interval between several minutes to a few hours of drips, while during dry periods, the interval was likely several days. In some cases, not enough volume was collected during the monthly period to run geochemical analyses.

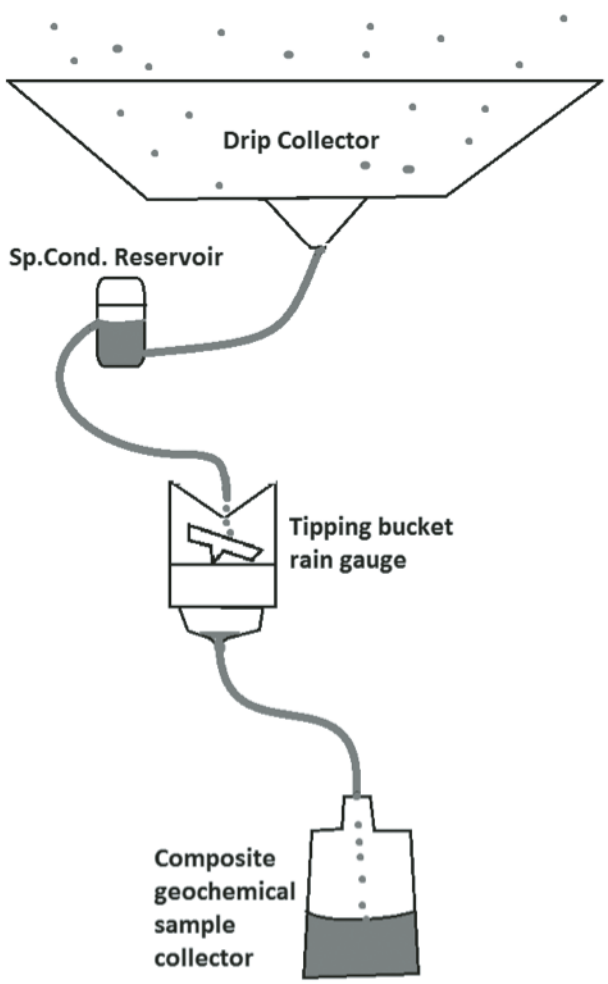

Figure 3. Schematic diagram of drip monitoring equipment and instrumentation. Sp.Cond.—specific conductance.

Analytical Methods

In the laboratory, water samples were filtered to 0.22 µm and separated into subsamples for analysis of cations, anions, alkalinity, and dissolved inorganic carbon (DIC) isotopes. Cation samples were preserved with HNO_3 and analyzed for Al, Ca, K, Mg, Na, Si, and Sr via inductively coupled plasma–atomic emission spectrometry (ICP-AES; Spectro ARCOS). Detection limits ranged from 0.003 to 0.009 mg/L, depending on the element. Anion samples were analyzed for Cl, NO_3, and SO_4 via ion chromatography (IC; Dionex DX-120); detection limits ranged from 0.1 to 0.5 mg/L, depending on the element. Replicate analyses for these parameters were run every 20 samples and were within 10%. Alkalinity was determined in the laboratory using gran titration (Radtke et al., 2012), and measurements were generally run within 24–48 h of sample collection, but on several occasions, this holding time was exceeded. A summary of the major ion data is presented in Table DR1.[1] Cation-anion balance errors often exceeded 10%, likely the consequence of exceeding the holding times for the alkalinity titrations.

Subsamples for stable carbon isotopes ($\delta^{13}C$) of total DIC were collected without headspace in vials sealed with low-diffusion butyl rubber septa. Analysis of the $\delta^{13}C$-DIC was conducted at the Reston Stable Isotope Laboratory of the U.S. Geological Survey according to the methodology described in Révész and Doctor (2014). Analytical error was within 0.2‰ (1 standard deviation).

Calculation of Precipitation Excess

Precipitation excess (also called water excess) was calculated by subtracting potential evapotranspiration (PET) from precipitation in weekly time steps, following the method of Genty and Deflandre (1998). The underlying assumption for calculating precipitation excess is that surface runoff is negligible, which is a reasonable assumption for the James Cave field site, where overland flow only occurs after extreme precipitation events. Similar assumptions and methods were used by Florea (2013) for the Redmond Creek aquifer, Kentucky.

PET was estimated using the Penman-Monteith method and a tall-grass reference, which adequately represents the pastures above and around the cave (ASCE-EWRI, 2005). A spreadsheet model (PMday) written by Snyder and Eching (2007) was used to perform daily PET calculations. Other required input data,

[1]GSA Data Repository Item 2015249, Box plots of selected ions and major ion concentrations, is available at www.geosociety.org/pubs/ft2015.htm, or on request from editing@geosociety.org or Documents Secretary, GSA, P.O. Box 9140, Boulder, CO 80301-9140, USA.

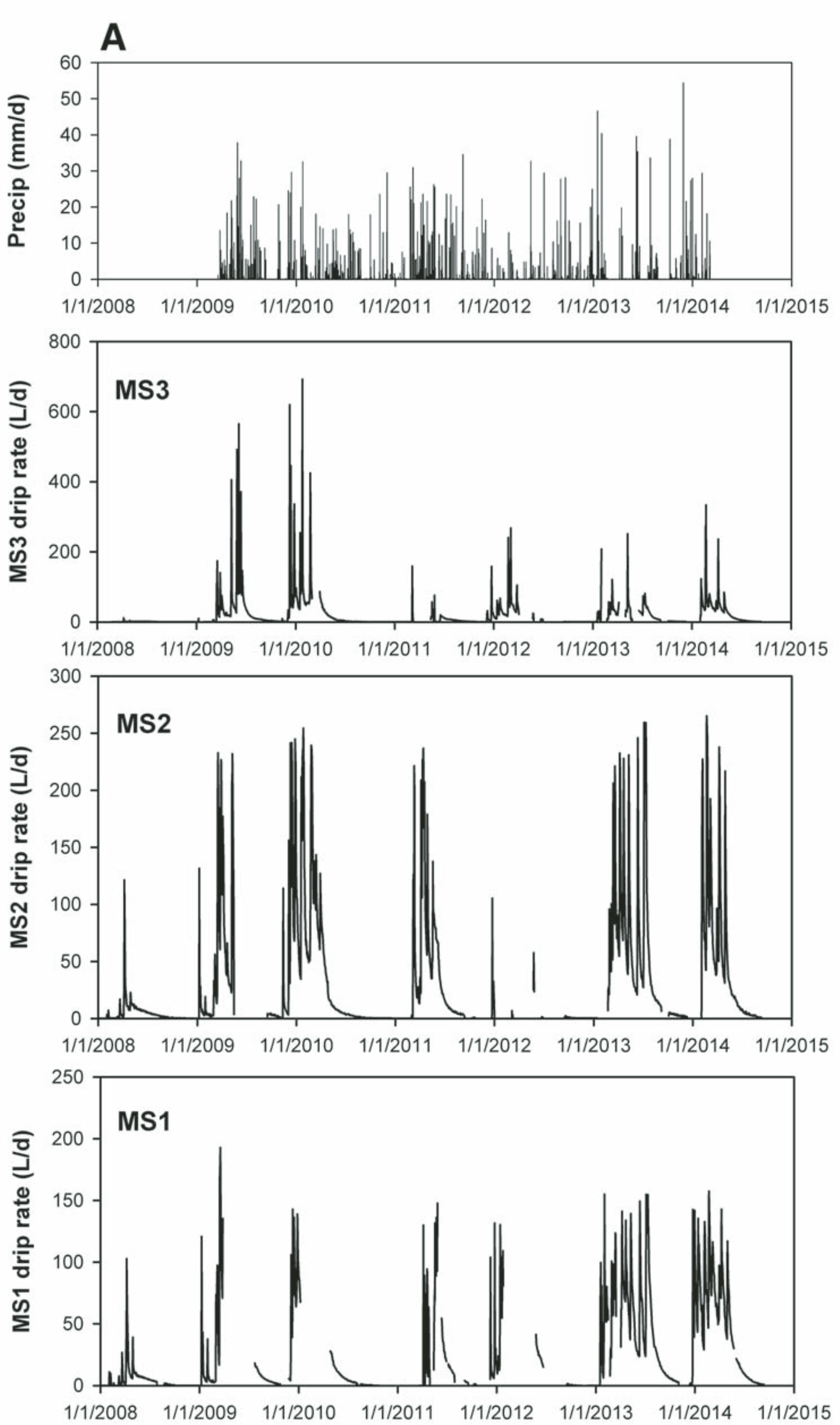

Figure 4 (*Continued on facing page*). (A) Hydrographs (daily sums; L/d) for drip sites (drip monitoring stations MS1–MS3) at James Cave. Note the different scales of drip rates for the three sites. Precipitation data were supplemented with data from Kentland Farms during times of rain gauge failure. Missing drip periods indicate equipment failure. (B) Summary of hydrologic seasons (Dry, Rch—recharge, Rcs—recession) for cave drips at James Cave for hydrologic year (HY) 2008 through 2014 based on the drip hydrographs. See text for definition of hydrologic years.

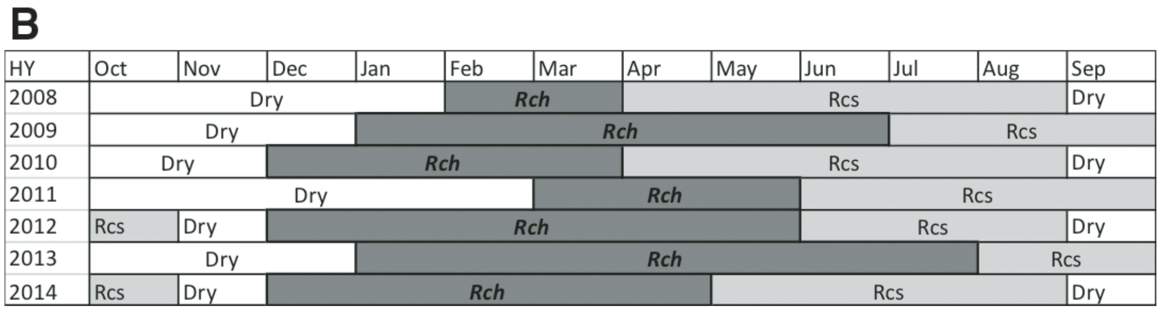

Figure 4 (*Continued*).

including daily maximum and minimum temperature, average wind speed, global solar radiation, and daily maximum and minimum relative humidity, were obtained from the Virginia Tech Kentland Farm (www.vaes.vt.edu/college-farm/weather/2014/weather2014.html).

RESULTS

Hydrology

Figure 4A shows the cave drip hydrographs and precipitation from late September 2007 to November 2014. Based on the drip hydrographs, the hydrologic record can be divided into three distinct periods: (1) a recharge period characterized by high drip rates and marked response to precipitation events; (2) a recession period showing the transition between the recharge and dry periods and during which there are no responses to precipitation events; and (3) a dry period during which there is no response to precipitation events, and the flow rate is at or near zero. We define the start of the hydrologic year (HY) as the start of the dry period, which generally begins in October). For example, HY2010 refers to the period October 2009–September 2010. This HY delineation corresponds with the U.S. Geologic Survey's definition of a hydrologic year, which starts October 1 and ends September 30.

Figure 4B contains a summary of the hydrologic seasons from 2008 to 2014. Over the period of record, the recharge season has started in December (HY2010, 2012, 2014), January (HY2009, 2013), February (HY2008), and March (HY2011). The duration of the recharge season has ranged from 2 mo (HY2008) to 7 mo (HY2013). The start and duration of the recession and dry periods also vary. The recession period has begun in April (HY2008, 2010), May (HY2014), June (JY 2011, 2012), and August (HY2013). Once it starts, the recession period can last from 3 to 5 mo. The start of the dry period has been more predictable (September–October), but its duration can vary from 1 to 6 mo.

Figure 5 shows the drip hydrograph for drip site MS2, as an example, with the calculated precipitation excess (Precipitation – PET > 0) and deficit (Precipitation – PET < 0) shown as a running average over the prior 13 wk interval and calculated at weekly time steps. The 13 wk interval provided the best fit between changes in precipitation excess and observed changes in drip hydrology (both wetting and drying), and it was selected from models that used data ranging from 2 to 20 wk prior PET running averages. Fit was evaluated by the times at which precipitation excess closely matched the observed recharge signals in the drip data, and, similarly, the periods of precipitation deficit correspond well with the recession and dry periods.

Discrete/Composite Hydrogeochemistry

Examples of ion box plots are shown for Ca and Sr in Figure 6 and illustrate increasing concentrations. Concentrations of these analytes increased with depth along a generalized flow path, from precipitation to soil water to drip water, reflecting increased rock-water interaction. Box plots of other ions (Mg, K, Na, Cl, SO_4, NO_3) are presented in the supplementary information (Fig. DR2 [see footnote 1]). These ions display more complex patterns because, in addition to having natural sources, they are also potentially sourced from road salt, fertilizer, and cow manure. Note that the farmer had deployed nutritional supplement feeders in the vicinity of lysimeter 3 (Soil3), located on the surface over drip site MS3 in the cave. Not only might these provide a source for the increased levels in some analytes (e.g., Cl), but they also cause cattle to concentrate in these areas for longer periods of time, resulting in greater potential contributions from livestock waste.

The hydrogeochemical signatures of drips also displayed temporal variations. For example, Ca concentrations showed seasonal oscillations at each of the drip sites (see Schreiber et al., 2015). The highest concentrations of Ca were generally observed in the late summer (August–September), and the lowest concentrations were observed in late fall and early winter (November–January). In contrast, Sr/Ca molar ratios were highest during the late fall and winter (November–January), and lowest during the summer to early fall (August–September; Fig. 7).

The δ^{13}C-DIC values were in the range expected for natural cave drip waters, varying between –15.2‰ and –0.8‰ (relative to Vienna Peedee belemnite [VPDB]; Fig. 7). For comparison, soil waters showed δ^{13}C-DIC values of –15.1‰ to –12.4‰, and they were more negative than the drip waters collected concurrently,

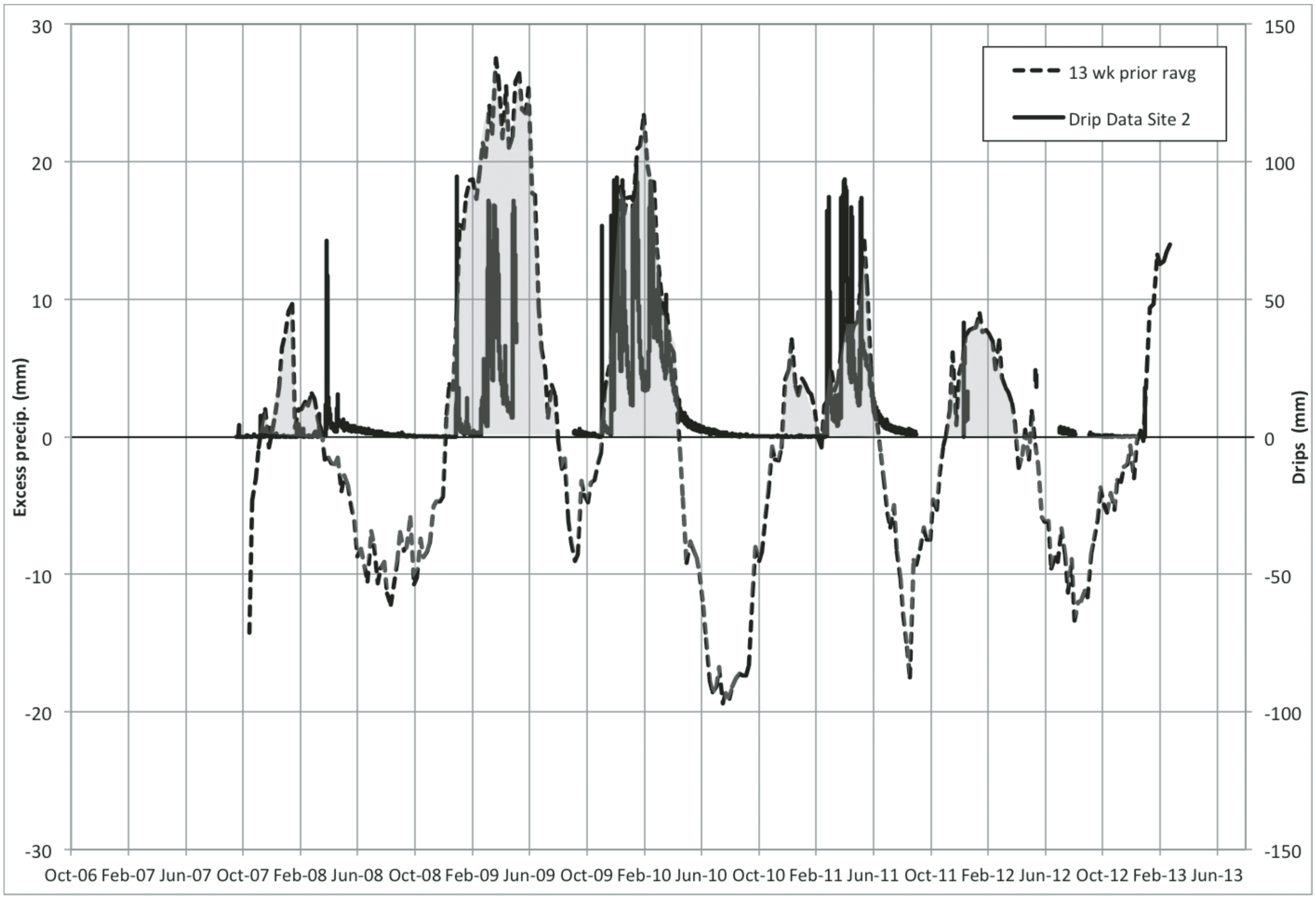

Figure 5. Precipitation excess (precipitation – potential evapotranspiration) calculated for October 2007 through February 2013 using 13 wk prior running average (ravg) at weekly time steps and overlain on the drip rate for drip monitoring station MS2. Gray shaded regions show excess; unshaded regions show deficit.

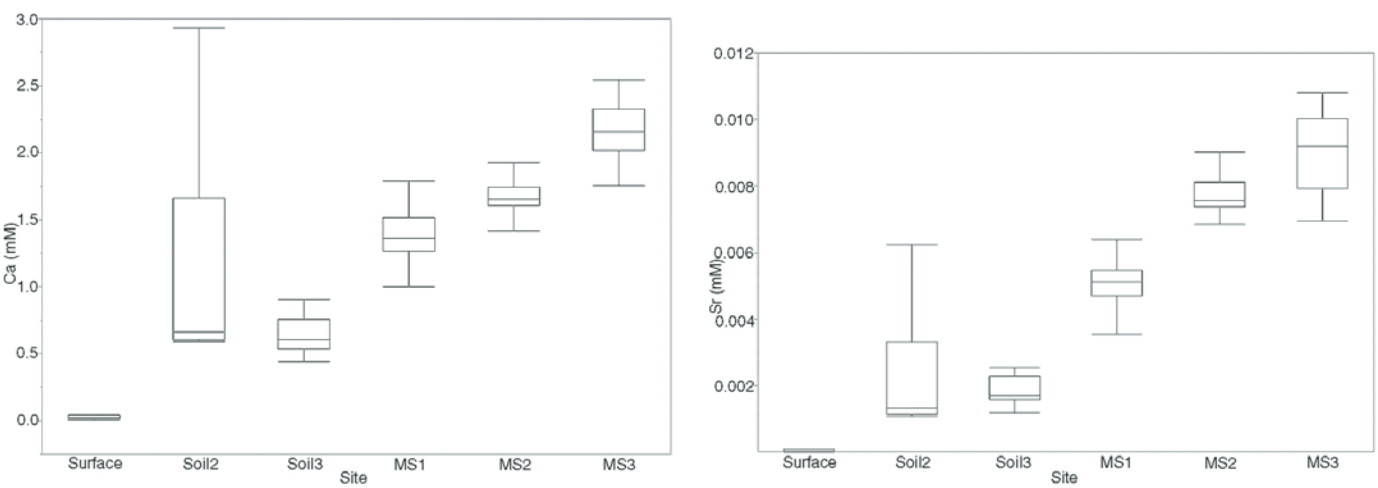

Figure 6. Box plots of Ca and Sr concentrations (m*M*) for surface (precipitation), Soil2 and Soil3 (soil water), and drip monitoring stations MS1–MS3 (drip water) sites. Number of samples: surface = 31, Soil2 = 9, Soil3 = 19, MS1 = 42, MS2 = 46, and MS3 = 39.

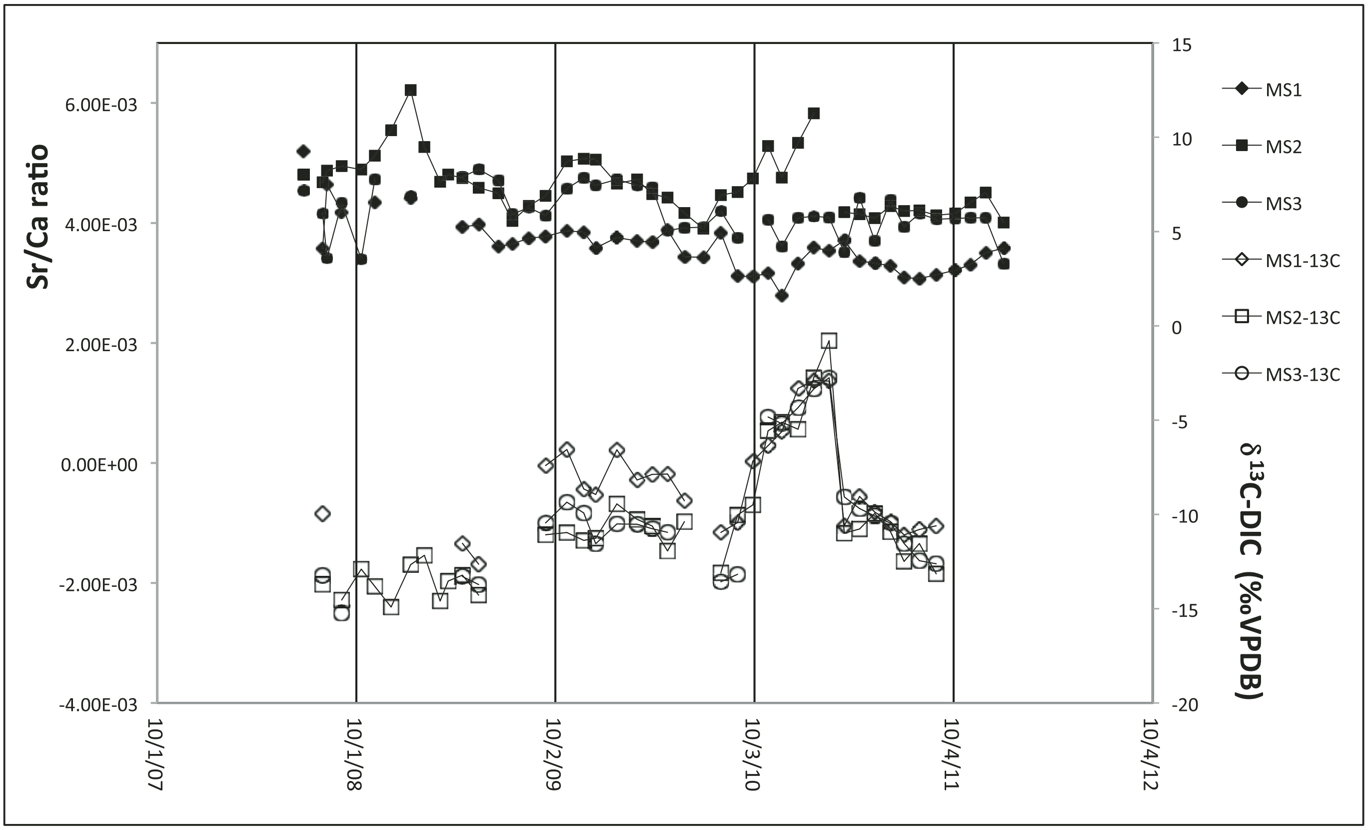

Figure 7. Sr/Ca ratios (left *y*-axis) and δ^{13}C-DIC (relative to Vienna Peedee belemnite [VPDB]; right *y*-axis) from monthly samples collected at drip monitoring stations (MS1–MS3) over time. DIC—dissolved inorganic carbon.

although it should be noted that due to volume limitations, we only have a few results for soil water. At all three drip sites, the δ^{13}C-DIC values increased from August 2010 to February 2011, corresponding with the dry season (see Fig. 4B).

Specific Conductance Time-Series Data

Time-series data of SpC from March 2011 to November 2014 are shown in Figure 8. Variation in SpC at each of the drip sites over the period of record can be separated into short-term perturbations (single recharge events) and longer-term (multiple month) trends. MS3 consistently had the highest SpC, while MS1 and MS2 generally had similar but lower SpC values. Worth noting is the decline in SpC in the fall season and the increase (more prominent at MS3) from spring to summer. Similar to the hydrologic record, the SpC record displays three main seasons (recharge, recession, dry period) during the hydrologic year. At all sites, initiation of the recharge season was accompanied by a distinct increase in base SpC ranging from 50 to 150 µS/cm. During the recharge season, SpC was the most variable, showing sharp decreases and fast recoveries that correspond to the initiation of drips and pulses following precipitation events.

Figure 9 shows the response in SpC at MS1–MS3 relative to the drip hydrograph of MS3 during the 2011–2012 recharge period. In the first recharge response observed (December 2011), there is a clear increase in SpC immediately after drips begin, followed by a sudden drop in SpC, and then an increase in SpC to a value 10%–25% higher than base conductivity during the dry period. For subsequent drip responses, only sudden drops in SpC followed by subsequent increases and a return to near preresponse values are observed. All three sites show similar responses. During the recession period, from May to August, SpC shows a steady increase and gradual plateau. During the dry period, from September to January, SpC gradually decreases, until the recharge season starts again.

DISCUSSION

Relationship between Drips and Precipitation

Drip rates at James Cave vary both seasonally and annually. The variability at all three sites shows similar trends related to and controlled by site-specific precipitation and evapotranspiration patterns, and the hydrogeologic properties of soils and the underlying epikarst. Precipitation- and evapotranspiration-dependent

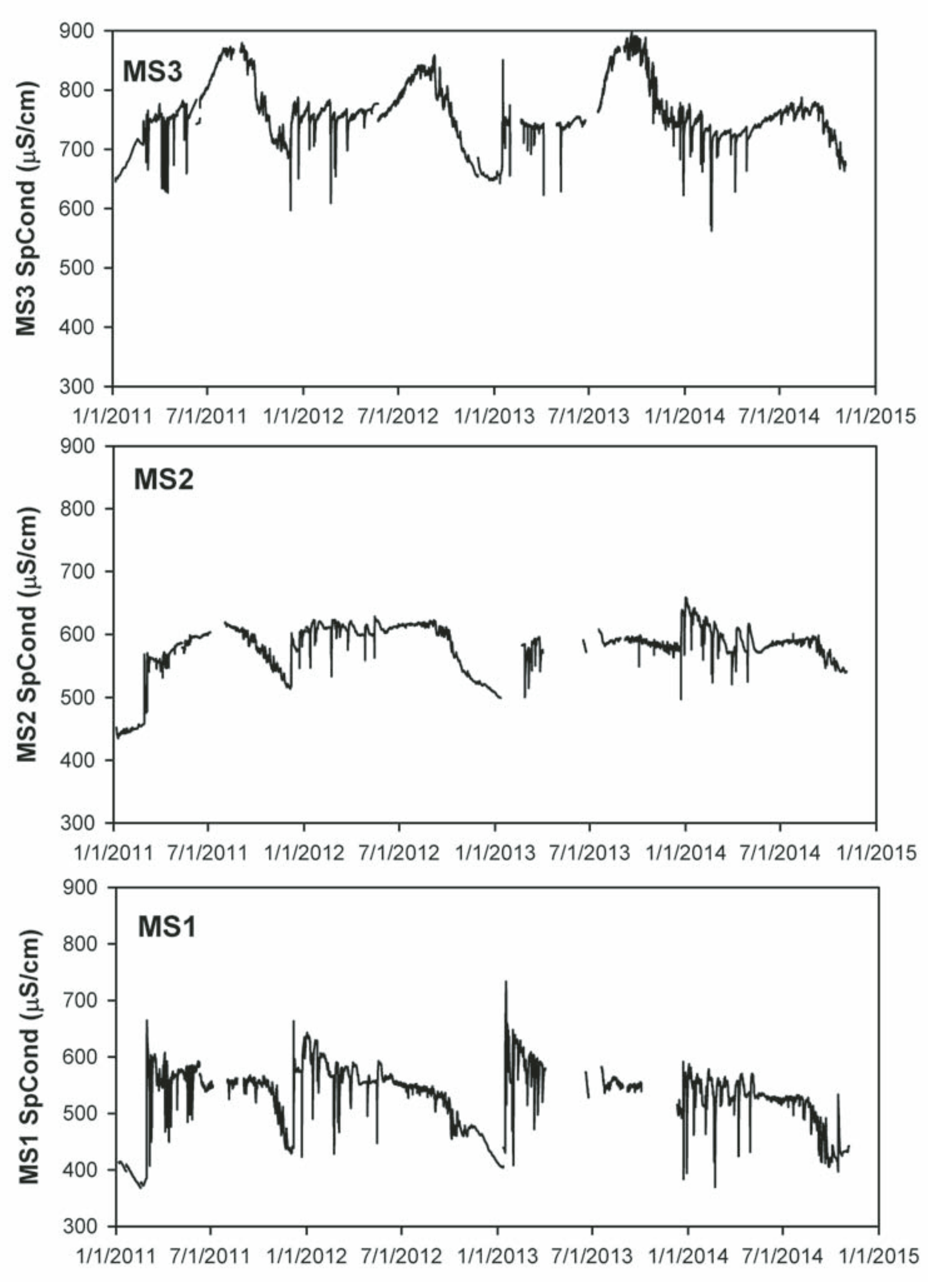

Figure 8. Specific conductance record (hourly mean; µS/cm) for drip monitoring stations (MS1–MS3) at James Cave from January 2011 to November 2014.

signals have been documented in other drip studies (Genty and Deflandre, 1998; Schwartz et al., 2013). Seasonal and annual drip-rate patterns correspond with periods of precipitation excess and deficit, which are controlled by the local climate, precipitation regime, and plant cover. This suggests that simple calculations of PET, in combination with precipitation data, can be used to predict the timing and duration of recharge, recession, and dry periods. This has also been reported by Gerard (2012), who developed predictive models of recharge response magnitude and occurrence at a site in the central Texas Edwards Plateau using precipitation, PET, and soil moisture data. Florea (2013) reached similar conclusions for karst in southeastern Kentucky using a combination of precipitation excess calculations and water isotope data.

Relationship between Drip Hydrology and Geochemistry

Comparison of hydrogeochemical records reveals strong correlations among the drip sites in the timing of initiation of and transitions between hydrologic seasons. At all sites, during initiation of the recharge season, an increase in SpC is observed with the first sharp increase in drip rate. Subsequent increases in

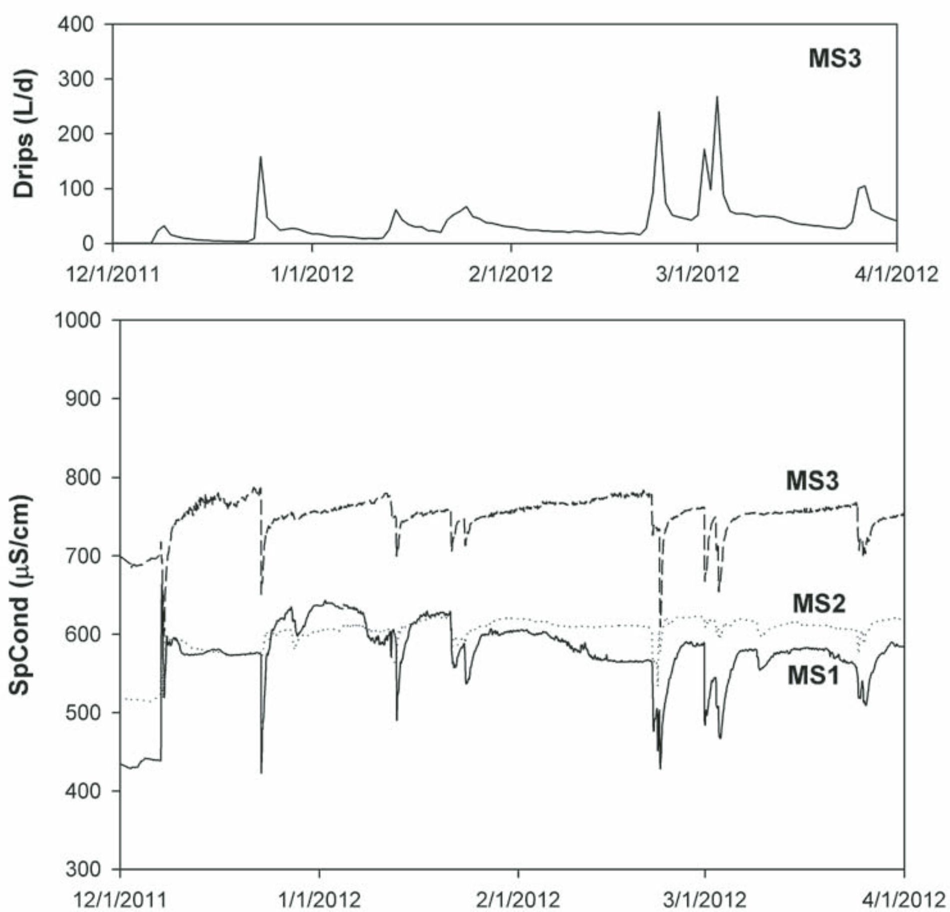

Figure 9. Drip data (daily sum in L/d) from MS3 (top) and specific conductance data (hourly mean; µS/cm) from drip monitoring stations MS1, MS2, and MS3 (bottom) for recharge period December 2011 to April 2012. Note the sharp decline in specific conductance in response to a drip event during this period.

drip rate are correlated with sharp decreases in SpC, suggesting a rapid influx of dilute water (i.e., recently infiltrated precipitation flowing through macropores). Genty and Deflandre (1998) noted a similar pattern of increased SpC in drip water associated with recharge, observing that SpC remained elevated during the recharge season. Our data show rapid decreases in SpC at all three sites in response to individual precipitation events throughout the recharge period, corresponding to the period of highest discharge. The only exceptions to this are the first responses of each season, during which the rapid decline is followed by a rapid increase in SpC toward values elevated 10%–25% above those in the dry period. The recession in drip rate abruptly changes slope within a couple of days after an event, returning to the pre-event slope but at drip rates higher than those preceding the event (see Fig. 9). The SpC value to which drips return following precipitation events during the recharge season varies between sites, with sites MS1 and MS2 showing an extended pulse of higher-conductivity water following precipitation events, while site MS3 slowly increased after each precipitation dilution event. These observations indicate that each precipitation event affects drip behavior in two ways: (1) an initial flush of meteoric or soil water that bypasses much of the epikarst, followed by (2) a more sustained increase in rate of discharge of water stored in the epikarst, presumably displaced by event water entering the system from the soil-bedrock interface.

During the hydrologic recession period, which coincides with the regional climatic summer, we observed a gradual increase in SpC in addition to increasing Ca, Sr, and HCO_3 concentrations in drip water. We attribute this pattern to increased water-rock interaction due to higher P_{CO_2} in the soil zone. During summer, increased biological activity produces higher CO_2 partial pressures within the epikarst (Yang et al., 2012), which increases calcite dissolution, resulting in increased Ca, Sr, and HCO_3 concentrations and higher SpC in drips. These observations are supported by results of other studies (e.g., Baldini et al., 2006) reporting increased Ca concentrations and calcite saturation indices in drip waters during the summer.

During the hydrologic dry period, there is a gradual decline of SpC in drips, in addition to decreasing Ca concentrations, and increasing Sr/Ca molar ratios. These patterns are suggestive of prior calcite precipitation, which removes Ca from drip water, resulting in lower SpC and an increase in the Sr/Ca ratio due to the preferential incorporation of Ca in precipitated calcite relative to Sr (Curti, 1999). Previous literature supports the use of Sr/Ca to infer prior calcite precipitation and has also been observed in cave drip waters (Genty and Deflandre, 1998;

Fairchild et al., 2000; Tooth and Fairchild, 2003; Musgrove and Banner, 2004; Wong et al., 2011).

The carbon isotope data can also be used to decipher geochemical processes. The data show increases in the δ^{13}C-DIC values in drips, coincident with increasing Sr/Ca ratios, during the August 2010 to February 2011 dry period. One potential cause of this increase is the kinetic isotopic fractionation associated with the outgassing of CO_2 from solution into the cave atmosphere. As CO_2 is exsolved from water, isotopic enrichment of the remaining HCO_3 is on the order of +10‰ at equilibrium (Mook et al., 1974; Zhang et al., 1995) and +14‰ under kinetic conditions (Marlier and O'Leary, 1984; Doctor et al., 2008). Such ^{13}C enrichment of DIC under conditions of calcite precipitation has been observed and modeled by others (e.g., Mickler et al., 2004; Spötl et al., 2005) and is also attributed to CO_2 loss from solution.

These increases in δ^{13}C-DIC cannot be accounted for by carbon isotopic equilibrium conditions of prior calcite precipitation. The equilibrium carbon isotopic fractionation between precipitated calcite and bicarbonate in solution is on the order of +1.3‰ ± 0.4‰ at 20 °C (Emrich et al., 1970); thus, the precipitated calcite is slightly enriched with respect to the solution and should result in lower δ^{13}C values of the remaining DIC. Although this effect diminishes with increasing rate of calcite precipitation (Turner, 1982), the result of calcite precipitation at carbon isotopic equilibrium should still be a net decrease in the δ^{13}C values of the remaining DIC. Instead, clear increases in the δ^{13}C-DIC values occur during periods of Sr and Mg enrichment and low flow rate of the drip waters, indicating prior calcite precipitation occurs under conditions far from carbon isotopic equilibrium.

We hypothesize that the strong degassing of CO_2 associated with prior calcite precipitation is a primary control on the observed δ^{13}C isotopic enrichment observed at all three drip sites during hydrologic dry periods in James Cave. The trend observed from the dry period of August 2010 to February 2011 abruptly ended in March 2011, when recharge caused rapid increases in drip rate, and the δ^{13}C of DIC decreased to below –10‰ at all three sites. This shift was likely influenced by the higher drip rate, as well as potentially greater CO_2 concentrations in the cave atmosphere during the warmer spring months, thus reducing CO_2 outgassing from the drip waters.

Conceptual Model of the Epikarst at James Cave

We derived a conceptual model of the epikarst at James Cave based on drip rate and specific conductivity results from our long-term study, shown schematically in Figure 10. Our data show the following key patterns:

(1) drip rate responsiveness to individual precipitation events is limited exclusively to the recharge season, when drip rates between precipitation events are also at their highest;
(2) onset of the recession period following the high-drip-rate period loosely corresponds to the onset of 13 wk running mean precipitation deficit, with SpC increasing during the recession period;
(3) onset of the dry season (when drip rates are constant and at their lowest values) occurs near the end of the summer growing season, and SpC of drip waters decreases during this period; and
(4) the transition from the dry season to the recharge season is abrupt, and it is accompanied by an increase in the SpC of drip waters to gradually rising levels, punctuated by short-duration negative SpC spikes associated with individual precipitation events. Drip rates between precipitation events also rise incrementally following precipitation events over the course of the recharge season.

Except in limited areas of surface bedrock exposure and in deeper dolines, precipitation must first move through the soil and the underlying epikarst before reaching the drips in the ceiling of the cave, the hydrology of which results from both soil and epikarst processes. Larger voids and vertical solutionally widened fissures within the epikarst are often filled with transported soil material, making the boundary between soil and epikarst hydrological domains vague and irregular. As pointed out by Tooth and Fairchild (2003), water moves through the soil column via diffuse porous media flow and through macropores. During precipitation events, downward flow within the macropores may bypass the adjacent soil matrix, producing a rapid response at the drips in the cave. However, increased drip rate response in the cave was only observed during the "recharge" season during the entire period of monitoring, no matter what the precipitation event. This implies that the epikarst has significant storage capacity that must be filled before flow events can propagate through the system and affect drips in the cave. The system is only completely connected by flow paths extending from the surface to the cave during the recharge season, and these flow paths are disconnected during the recession and dry hydrologic seasons.

One way to explain this behavior is that the bedrock voids within the epikarst function as a series of cascading and leaking reservoirs that fill from the top and drain from the bottom. These voids provide intermediate storage capacity fed by discharge from the soil zone, which develops a seasonally saturated zone at its base and within sediment-filled voids and fissures that extend into the bedrock (Fig. 10). Although discharge from the soil zone is primarily controlled by porous media flow, macropores exist within it that can be significant bypass routes for water to rapidly enter the epikarst following precipitation events. We now discuss what we propose is happening between the land surface and the cave over the course of a hydrologic year, starting with the dry season and continuing through the recharge and, finally, recession seasons. Figure 10 illustrates this conceptual model.

By late summer to early fall, most water has drained out of the bedrock through the drips in the cave, and the seasonally saturated zone near the top of the epikarst has been depleted of moisture due to evapotranspiration from plant growth. Thus, at the start of the dry season, the drips in the cave have become completely disconnected from the influence of surface precipitation events. Calcite precipitates in the air-filled portions of the epikarst, driven by CO_2 outgassing induced by air exchange between

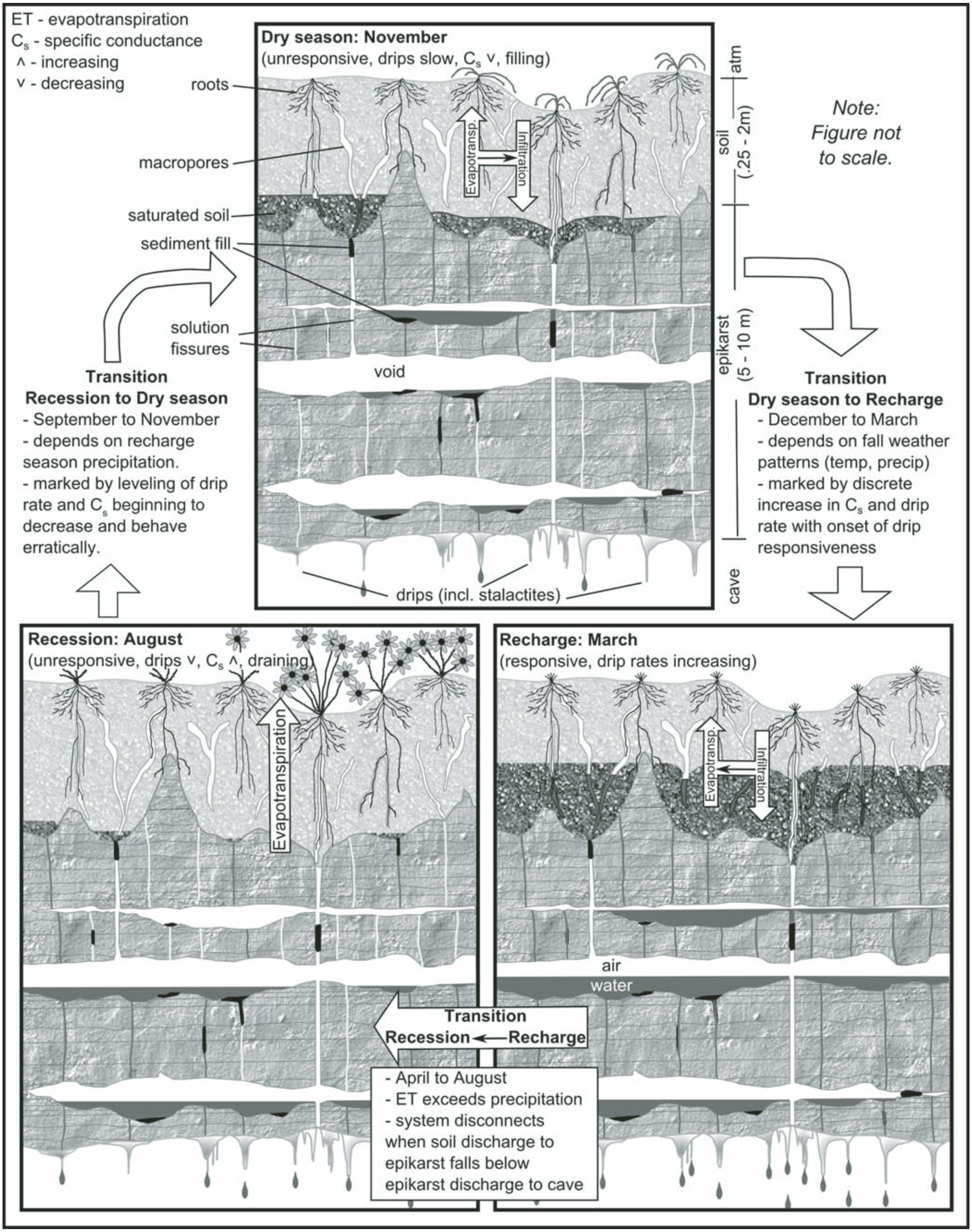

Figure 10. Conceptual model of epikarst at James Cave, Virginia, showing major processes occurring in the recharge, recession, and dry hydrologic seasons. ET—evapotranspiration; Cs—specific conductance; ^ = increasing; ᵛ = decreasing.

the cave and surface atmospheres as the surface air temperature cools below cave air temperature, and the cave ventilates. This results in a progressive reduction of SpC values, lower Ca concentrations, higher Sr/Ca ratios, and increasing δ^{13}C-DIC values in drips.

Infiltration via macropores and piston flow likely occur in response to precipitation events during the dry season, but these events are not observed at the cave drips because the newly added water replenishes the soil moisture deficit accumulated over the growing season, and any bypass flows through macropores are intercepted by the bedrock void reservoirs in the epikarst. As the dry season continues into autumn, infiltration begins to exceed evapotranspiration, and both the soil matrix and bedrock epikarst reservoirs begin to refill. Once the soil moisture deficit is overcome to the point where the matric potential exceeds atmospheric pressure, water can be efficiently transmitted through the seasonally saturated zone into the bedrock. The seasonally saturated zone thickens, while the bedrock voids in the epikarst fill from the top down, eventually to the point of allowing rapid transmission of recharge pulses from the surface to the drips. The drip water and SpC records clearly show that once the critical threshold of epikarst storage is surpassed, a single precipitation event can produce (1) a sharp increase in drip rate, (2) an increase of 100–200 µS/cm in SpC, and (3) the onset of drip responsiveness that characterizes the recharge season.

The abrupt increase in SpC that results with the initial drip response to precipitation at the start of the recharge season is the result of mineralized water that has been held within the fast flow paths in the epikarst being expelled at the drips. Following subsequent precipitation events over the course of the recharge season, less mineralized water, transmitted rapidly from the surface along bypass flow paths (macropores and vertical solution fissures), is reflected by decreases in SpC associated with short-lived (a day or two) rapid discharge spikes before a return to pre-event levels. Precipitation events increase the thickness of the saturated soil zone, providing the soil moisture that drives relatively high drip rates between precipitation events.

During the recharge season, prior precipitation of calcite in the epikarst ceases or is greatly reduced due to discharge of calcite-undersaturated, CO_2-enriched water from the saturated zone at the soil-epikarst interface. Moreover, the base of the seasonally saturated zone is the region of most intense rock dissolution within the epikarst, since it (1) is where the carbonate-undersaturated soil water first meets the carbonate bedrock upon infiltration, (2) is a region of significant CO_2 production, and (3) has sufficient residence time for enhanced water-rock interaction.

Evapotranspiration increases over the course of the recharge season, so less water reaches the saturated base of the soil (which itself is likely directly affected by plant transpiration). Discharge from the soil to the epikarst falls below discharge from epikarst to the cave, the system becomes hydrologically disconnected, and precipitation events no longer propagate through the system. This sequence of events initiates the recession season.

During the recession season, the epikarst drains from below, as evidenced by the exponential decay in drip rate. SpC values increase as the water-rock contact time increases without dilution due to influxes of meteoric water, and as CO_2 partial pressure in the soil increases. Temperatures on the surface are higher than those in the cave, retarding circulation of air in the epikarst and maintaining a high-CO_2 cave atmosphere. Eventually, drips reach a minimum discharge, and the increased air-filled voids in the epikarst allow reduction in CO_2 levels, facilitated by convection-driven circulation as autumn temperatures fall below those in the epikarst. Calcite precipitation initiates, and SpC values decrease, marking the onset of the dry season.

CONCLUSIONS

In this study, we present a high-resolution data set of drip hydrology and geochemistry collected from James Cave, Virginia. Results indicate a strong seasonality of recharge, lasting up to 6 mo during wet years and as little as 2 mo during dry years. Using combined hydrologic and geochemical data sets, we derive a conceptual model for the influence of hydrologic processes in the epikarst on geochemical signatures of drips, which both affect recharge to the underlying karst aquifer. Results of this study show that multiyear, high-resolution monitoring provides a deeper understanding of fine-scale processes that exert important controls on recharge to karst aquifers.

ACKNOWLEDGMENTS

We gratefully acknowledge funding from the Virginia Water Resources Research Center, the U.S. Geological Survey/National Institutes for Water Resources, the Cave Conservancy of the Virginias, the Geological Society of America, and the Virginia Tech Department of Geosciences. We thank David Culver for discussions about study design and data collection; Don Rimstidt for geochemical insight; Tom Malabad for conducting the cave survey; and Stuart Hyde, Heather Scott, Matthew Blower, Ariel Brown, Sara Fleetwood, and members of the Virginia Polytechnic Institute Cave Club for valuable assistance in the cave. Thanks also to the Ferrell family for allowing access to James Cave and to the staff at the Virginia Tech Kentland Farm for providing additional weather data. Insightful comments from Art Palmer, John Nimmo, and two anonymous reviewers greatly improved the manuscript.

REFERENCES CITED

American Society of Civil Engineers–Environmental and Water Resources Institute (ASCE-EWRI), 2005, The ASCE Standardized Reference Evapotranspiration Equation: Technical Committee (Allen, R.G., Walter, I.A., Elliot, R.L., Howell, T.A., Itenfisu, D., Jensen, M., and Snyder, R.L.) Report to the Environmental and Water Resources Institute of the American Society of Civil Engineers from the Task Committee on Standardization of Reference Evapotranspiration: Reston, Virginia, American Society of Civil Engineers, 100 p.

AquaticInformatics, 2011, AQUARIUS 3.0 R3, 1032: Vancouver, British Columbia, AquaticInformatics, http://aquaticinformatics.com/ (accessed 2014).

Aquilina, L., Ladouche, B., and Dorfliger, N., 2006, Water storage and transfer in the epikarst of karstic systems during high flow periods: Journal of Hydrology, v. 327, no. 3–4, p. 472–485.

Bakalowicz, M.J., 2004, The epikarst, the skin of karst, *in* Jones, W.K., Culver, D.C., and Herman, J.S., eds., Epikarst: Karst Waters Institute Special Publication 9, p. 16–22.

Baker, A., Genty, D., and Fairchild, I.J., 2000, Hydrological characterisation of stalagmite dripwaters at Grotte de Villars, Dordogne, by the analysis of inorganic species and luminescent organic matter: Hydrology and Earth System Sciences, v. 4, no. 3, p. 439–449, doi:10.5194/hess-4-439-2000.

Baldini, J.U.L., McDermott, F., and Fairchild, I.J., 2006, Spatial variability in cave drip water hydrochemistry: Implications for stalagmite paleoclimate records: Chemical Geology, v. 235, no. 3–4, p. 390–404.

Baldini, J.U.L., McDermott, F., Baldini, L.M., Ottley, C.J., Linge, K.L., Clipson, N., and Jarvis, K.E., 2012, Identifying short-term and seasonal trends in cave drip water trace element concentrations based on a daily-scale automatically collected drip water dataset: Chemical Geology, v. 330–331, p. 1–16, doi:10.1016/j.chemgeo.2012.08.009.

Bartholomew, M.J., 1987, Structural evolution of the Pulaski thrust system, southwestern Virginia: Geological Society of America Bulletin, v. 99, no. 4, p. 491–510, doi:10.1130/0016-7606(1987)99<491:SEOTPT>2.0.CO;2.

Bingham, E., 1991, The physiographic provinces of Virginia: The Virginia Geographer, v. 23, no. 2, p. 19–32.

Curti, E., 1999, Coprecipitation of radionuclides with calcite: Estimation of partition coefficients based on a review of laboratory investigations and geochemical data: Applied Geochemistry, v. 14, no. 4, p. 433–445, doi:10.1016/S0883-2927(98)00065-1.

Doctor, D.H., Kendall, C., Sebestyen, S.D., Shanley, J.B., Ohte, N., and Boyer, E.W., 2008, Carbon isotope fractionation of dissolved inorganic carbon (DIC) due to outgassing of carbon dioxide from a headwater stream: Hydrological Processes, v. 22, no. 14, p. 2410–2423, doi:10.1002/hyp.6833.

Eagle, S.D., 2013, Analysis of Hydrologic and Geochemical Time Series Data at James Cave, Virginia: Implications for Epikarst Influence on Recharge [M.S. thesis]: Blacksburg, Virginia, Department of Geosciences, Virginia Tech, 113 p.

Emrich, K., Ehhalt, D., and Vogel, J., 1970, Carbon isotope fractionation during the precipitation of calcium carbonate: Earth and Planetary Science Letters, v. 8, no. 5, p. 363–371, doi:10.1016/0012-821X(70)90109-3.

Fairchild, I.J., and McMillan, E.A., 2007, Speleothems as indicators of wet and dry periods: International Journal of Speleology, v. 36, no. 2, p. 69–74, doi:10.5038/1827-806X.36.2.2.

Fairchild, I.J., Borsato, A., Tooth, A.F., Frisia, S., Hawkesworth, C.J., Huang, Y.M., McDermott, F., and Spiro, B., 2000, Controls on trace element (Sr-Mg) compositions of carbonate cave waters: Implications for speleothem climatic records: Chemical Geology, v. 166, no. 3–4, p. 255–269.

Field, M.S., 2002, A Lexicon of Cave and Karst Terminology with Special Reference to Environmental Karst Hydrology: U.S. Environmental Protection Agency Office of Research and Development (ORD) Report EPA/600/R-02/003, 221 p.

Florea, L.J., 2013, Selective recharge and isotopic composition of shallow groundwater within temperate, epigenic carbonate aquifers: Journal of Hydrology, v. 489, p. 201–213, doi:10.1016/j.jhydrol.2013.03.008.

Genty, D., and Deflandre, G., 1998, Drip flow variations under a stalactite of the Pere Noel cave (Belgium): Evidence of seasonal variations and air pressure constraints: Journal of Hydrology, v. 211, no. 1–4, p. 208–232.

Gerard, B.R., 2012, Effects of Environmental Parameters and Precipitation Dynamics on Infiltration and Recharge into the Trinity Aquifer of Central Texas [M.S. thesis]: San Marcos, Texas, Department of Biology, Texas State University–San Marcos, 63 p.

Gregory, L., Wilcox, B., Shade, B., Munster, C., Owens, K., and Veni, G., 2009, Large-scale rainfall simulation over shallow caves on karst shrublands: Ecohydrology, v. 2, p. 72–80, doi:10.1002/eco.41.

Kazahaya, K., and Yasuhara, M., 1994, A hydrogen isotopic study of spring waters in Mt. Yatsugatake, Japan: Application to groundwater recharge and flow processes: Journal of Japanese Association of Hydrological Sciences, v. 24, p. 107–119.

Klimchouk, A., 2003, Towards defining, delimiting and classifying epikarst: Its origin, processes and variants of geomorphic evolution, *in* Jones, W.K., Culver, D.C., and Herman, J.S., eds., Epikarst: Karst Waters Institute Special Publication 9, p. 23–35.

Marlier, J.F., and O'Leary, M.H., 1984, Carbon kinetic isotope effects on the hydration of carbon dioxide and the dehydration of bicarbonate ion: Journal of the American Chemical Society, v. 106, no. 18, p. 5054–5057, doi:10.1021/ja00330a003.

McDonald, J., and Drysdale, R., 2007, Hydrology of cave drip waters at varying bedrock depths from a karst system in southeastern Australia: Hydrological Processes, v. 21, no. 13, p. 1737–1748, doi:10.1002/hyp.6356.

Mickler, P.J., Banner, J.L., Stern, L., Asmerom, Y., Edwards, R.L., and Ito, E., 2004, Stable isotope variations in modern tropical speleothems: Evaluating equilibrium vs. kinetic isotope effects: Geochimica et Cosmochimica Acta, v. 68, no. 21, p. 4381–4393, doi:10.1016/j.gca.2004.02.012.

Mook, W., Bommerson, J., and Staverman, W., 1974, Carbon isotope fractionation between dissolved bicarbonate and gaseous carbon dioxide: Earth and Planetary Science Letters, v. 22, no. 2, p. 169–176, doi:10.1016/0012-821X(74)90078-8.

Musgrove, M., and Banner, J.L., 2004, Controls on the spatial and temporal variability of vadose dripwater geochemistry: Edwards Aquifer, central Texas: Geochimica et Cosmochimica Acta, v. 68, no. 5, p. 1007–1020, doi:10.1016/j.gca.2003.08.014.

Pape, J.R., Banner, J.L., Mack, L.E., Musgrove, M., and Guilfoyle, A., 2009, Controls on oxygen isotope variability in precipitation and cave drip waters, central Texas, USA: Journal of Hydrology, v. 385, no. 1–4, p. 203–215.

Perrin, K., Jeannin, P.Y., and Zwahlen, F., 2003, Epikarst storage in a karst aquifer: A conceptual model based on isotopic data, Milandre test site, Switzerland: Journal of Hydrology, v. 279, no. 1–4, p. 106–124.

Radtke, D.B., Wilde, F.D., Davis, J.V., and Popowski, T.J., 2012, Alkalinity and acid neutralizing capacity (version 4.0), *in* Rounds, S.A., ed., National Field Manual for the Collection of Water-Quality Data: U.S. Geological Survey Techniques of Water-Resources Investigations 9.

Révész, K.M., and Doctor, D.H., 2014, Automated Determination of the Stable Carbon Isotopic Composition ($\delta^{13}C$) of Total Dissolved Inorganic Carbon (DIC) and Total Nonpurgeable Dissolved Organic Carbon (DOC) in Aqueous Samples: RSIL Lab Codes 1851 and 1852: U.S. Geological Survey Techniques and Methods Book 10, 38 p.

Schreiber, M.E., Schwartz, B.F., Orndorff, W.D., Doctor, D.H., Eagle, S.D., and Gerst, J.D., 2015, Instrumenting caves to collect hydrologic and geochemical data: Example from James Cave, Virginia, *in* Younos, T., and Parece, T., eds., Advances in Watershed Science and Assessment: New York, Springer, p. 205–231, doi:10.1007/978-3-319-14212-8_8.

Schultz, A.P., and Bartholomew, M.J., 2009, Geologic Map of the Radford North Quadrangle, Virginia: Virginia Division of Mineral Resources Digital Open-File Report OFR-09-01, scale 1:24,000.

Schwartz, B.F., Schwinning, S., Gerard, B., Kukowski, K.R., Stinson, C.L., and Dammeyer, H.C., 2013, Using hydrogeochemical and ecohydrologic responses to understand epikarst process in semi-arid systems, Edwards Plateau, Texas, USA: Acta Carsologica, v. 42, no. 2–3, p. 315–325.

SERCC, 2012, Historical Climate Summaries for Virginia: Chapel Hill, North Carolina, The University of North Carolina, www.sercc.com/climateinfo/historical/historical_va.html (accessed 1 November 2014).

Sheffer, N.A., Cohen, M., Morin, E., Grodek, T., Gimburg, A., Magal, E., Gvirtzman, H., Nied, M., Isele, D., and Frumkin, A., 2011, Integrated cave drip monitoring for epikarst recharge estimation in a dry Mediterranean area, Sif Cave, Israel: Hydrological Processes, v. 25, no. 18, p. 2837–2845, doi:10.1002/hyp.8046.

Sherwin, C.M., and Baldini, J.U.L., 2011, Cave air and hydrological controls on prior calcite precipitation and stalagmite growth rates: Implications for palaeoclimate reconstructions using speleothems: Geochimica et Cosmochimica Acta, v. 75, no. 14, p. 3915–3929, doi:10.1016/j.gca.2011.04.020.

Smart, P.L., and Friederich, H., 1987, Water movement and storage in the unsaturated zone of a maturely karstified carbonate aquifer, Mendip Hills, England, *in* Proceedings of the Conference on Environmental Problems in Karst Terranes and Their Solutions: Dublin, Ohio, National Water Well Association, p. 59–87.

Snyder, R.L., and Eching, S., 2007, PMday: http://biomet.ucdavis.edu/evapotranspiration.html (accessed 1 Nov. 2014).

Spötl, C., Fairchild, I.J., and Tooth, A., 2005, Cave air control on dripwater geochemistry, Obir Caves (Austria): Implications for speleothem deposition in dynamically ventilated caves: Geochimica et Cosmochimica Acta, v. 69, no. 10, p. 2451–2468, doi:10.1016/j.gca.2004.12.009.

Tooth, A.F., and Fairchild, I.J., 2003, Soil and karst aquifer hydrological controls on the geochemical evolution of speleothem-forming drip waters, Crag Cave, southwest Ireland: Journal of Hydrology, v. 273, no. 1–4, p. 51–68.

Turner, J.V., 1982, Kinetic fractionation of carbon-13 during calcium carbonate precipitation: Geochimica et Cosmochimica Acta, v. 46, no. 7, p. 1183–1191, doi:10.1016/0016-7037(82)90004-7.

U.S. Department of Agriculture–Natural Resources Conservation Service (USDA-NRCS), 2006, Web Soil Survey: http://websoilsurvey.nrcs.usda.gov/app/WebSoilSurvey.aspx (accessed 1 November 2014).

Williams, P.W., 1983, The role of the subcutaneous zone in karst hydrology: Journal of Hydrology, v. 61, no. 1–3, p. 45–67.

Williams, P.W., 2008, The role of the epikarst in karst and cave hydrogeology: A review: International Journal of Speleology, v. 37, no. 1, p. 1–10, doi:10.5038/1827-806X.37.1.1.

Wong, C.I., Banner, J.L., and Musgrove, M., 2011, Seasonal dripwater Mg/Ca and Sr/Ca variations driven by cave ventilation: Implications for and modeling of speleothem paleoclimate records: Geochimica et Cosmochimica Acta, v. 75, no. 12, p. 3514–3529, doi:10.1016/j.gca.2011.03.025.

Yang, R., Liu, Z., Zeng, C., and Zhao, M., 2012, Response of epikarst hydrochemical changes to soil CO_2 and weather conditions at Chenqi, Puding, SW China: Journal of Hydrology, v. 468–469, p. 151–158, doi:10.1016/j.jhydrol.2012.08.029.

Zhang, J., Quay, P., and Wilbur, D., 1995, Carbon isotope fractionation during gas-water exchange and dissolution of CO_2: Geochimica et Cosmochimica Acta, v. 59, no. 1, p. 107–114, doi:10.1016/0016-7037(95)91550-D.

Manuscript Accepted by the Society 17 April 2015